Slit design for efficient and accurate MTF measurement at megavoltage x-ray energies

Amit Sawant, Larry Antonuk,[a] and Youcef El-Mohri
Department of Radiation Oncology, University of Michigan, Ann Arbor, Michigan 48103

(Received 24 June 2006; revised 24 January 2007; accepted for publication 26 February 2007; published 18 April 2007)

Empirical determination of the modulation transfer function (MTF) for analog and digital megavoltage x-ray imagers is a challenging task. The most common method used to determine MTF at megavoltage x-ray energies employs a long, narrow slit formed by two parallel, metal blocks in order to form a "slit beam." In this work, a detailed overview of some of the important considerations of slit design is presented. Based on these considerations, a novel, compact slit, using 19 cm thick tungsten blocks, was designed. The prototype slit was configured to attach to the accessory slot of the gantry of a linear accelerator, which greatly simplified the measurement process. Measurements were performed to determine the presampling MTF at 6 MV for an indirect detection active matrix flat panel imager prototype previously developed for megavoltage imaging applications. In addition, the effects of two important slit design parameters, material type and thickness, on the accuracy of MTF determination were investigated via a Monte Carlo-based theoretical study. Empirically determined MTFs obtained from the prototype slit closely match those from an earlier, less compact slit design based on 40 cm thick steel blocks. The results of the Monte Carlo-based theoretical studies indicate that the prototype slit achieves close-to-ideal performance in terms of accurately determining the MTF by virtue of practically 100% beam attenuation in regions other than the slit gap. Furthermore, the theoretical results suggest that it may be possible to achieve even further reductions in slit thickness without compromising measurement accuracy. © *2007 American Association of Physicists in Medicine.* [DOI: 10.1118/1.2717405]

Key words: modulation transfer function, MTF measurement, slit method, megavoltage x-ray imaging, portal imaging

I. INTRODUCTION

Modulation transfer function (MTF) is the metric most widely used to characterize the spatial resolution properties of linear (or linearizable) and shift-invariant (or periodically shift-invariant) x-ray imaging systems. The one-dimensional (1D) or two-dimensional (2D) MTF of an imaging system is determined from the absolute value of the Fourier transform of the 1D or 2D impulse response [the line spread function (LSF) or the point spread function, respectively] of the system. In particular, one-dimensional MTF is the preferred metric for characterizing spatial resolution properties and calculating frequency-dependent detective quantum efficiency of diagnostic and megavoltage x-ray imaging systems.[1]

Empirical determination of the MTF for megavoltage imagers is usually performed by employing a method involving the use of a narrow slit formed by two equally-sized blocks of a high-density material, typically, steel or tungsten, separated by thin shims. Descriptions of the techniques used for MTF measurements at megavoltage energies using the slit method, as well as an overview of some of the technical considerations, can be found in early work by Droege *et al.*,[2] and subsequent work by Munro *et al.*[3–5] MTF measurements based on this technique have also been reported by our group[6–8] and others[9–12] for performance characterization of prototype and commercially available megavoltage imaging systems.

The high energies encountered in megavoltage x-ray imaging (typically 6 to 25 MV), coupled with effects such as head scatter from the linear accelerator and background scatter, result in an environment that presents significant challenges to performing accurate measurements. Consequently, building a slit for LSF measurements performed under such conditions requires careful selection of a variety of design parameters such as dimensions and material of the slit blocks, width of the slit gap, distance from the source, etc. In previously reported studies, there has been wide variation in the choice of material and dimensions for slit designs—ranging from a design based on 1.6 cm thick tungsten blocks[2] to slits formed by 60 cm thick steel blocks.[4,9] While the thickest of these slits are very likely to yield accurate results, the use of such massive blocks gives rise to practical difficulties arising from the weight and bulkiness of the slit that negatively impact the ease and feasibility of empirical determination of the MTF. Consequently, it is useful and interesting to examine whether slits can be made significantly more compact while simultaneously maintaining a high degree of measurement accuracy. Such designs could prove to be invaluable for tasks ranging from the characterization of novel megavoltage imager prototypes to performing quality assurance on clinical imagers.

In this work, we first present a detailed overview of some of the important technical aspects of slit design for LSF measurements performed under megavoltage x-ray imaging con-

ditions. (Note that, hereafter, the term "slit" will be used to refer to the entire structure comprising the two metal blocks, while the gap between the two blocks will be referred to as the "slit gap.") Based on these considerations, a novel, compact megavoltage imaging slit, that can be inserted into the accessory slot of a linear accelerator gantry, was constructed. Design details of this slit are discussed and MTF measurements at 6 MV of a phosphor screen-based active matrix flat panel imager (AMFPI) electronic portal imaging device (EPID) using the prototype slit are compared with those previously published by our group, obtained under similar imaging conditions using an earlier, less compact slit design.[6] Finally, a systematic, Monte Carlo-based investigation is presented in order to examine the tradeoff between compactness of slit design and the accuracy of MTF measurements. These studies consider materials (steel and tungsten) and thicknesses (5 to 40 cm) that are commonly used to construct slits for megavoltage imaging.[2–7,9–11]

II. TECHNICAL BACKGROUND

The slit method can be used for the determination of the LSF (and thereafter, the MTF) of analog as well as digital x-ray imaging systems. Details of these techniques may be found elsewhere.[10,13] While the analytical procedures involved in LSF determination of these two types of systems are significantly different, the aspects of slit design examined in the present study are common to both.

In order to facilitate the discussion that follows, a schematic cross-sectional view of a slit placed under a megavoltage x-ray source is shown in Fig. 1. For simplicity, the megavoltage x-ray source is considered to be a point source. The straight-line trajectories of incident megavoltage x rays can be divided into three groups. X rays that are incident at angles less than ε with respect to the central axis of the beam pass unattenuated through the slit gap. X rays that are incident at angles less than θ but greater than ε, pass partially through the block edges that form the slit gap. Finally, x rays incident at angles greater than θ, but less than ϕ, pass through the entire thickness of the block. Based on the geometry shown in Fig. 1, the three angles can be calculated from

$$\phi = \tan^{-1}\left(\frac{F/2}{D}\right), \tag{1}$$

$$\theta = \tan^{-1}\left(\frac{G/2}{D-T}\right), \tag{2}$$

$$\varepsilon = \tan^{-1}\left(\frac{G/2}{D}\right), \tag{3}$$

where G is the width of the slit gap, D is the distance between the source and the exit surface of the slit, and F is the width of the x-ray exit surface of the slit. (For example, in the case of a measurement geometry using a slit having dimensions 40 cm (thick) $\times$6.5 cm$\times$6.5 cm and a slit gap width of 0.01 cm, positioned at a source to exit surface distance of 130 cm, the approximate values of ϕ, θ, and ε will be 1.432°, 0.003°, and 0.002°, respectively.) As explained in the following sections, the signal contribution from each group of x rays affects LSF measurement in different ways.

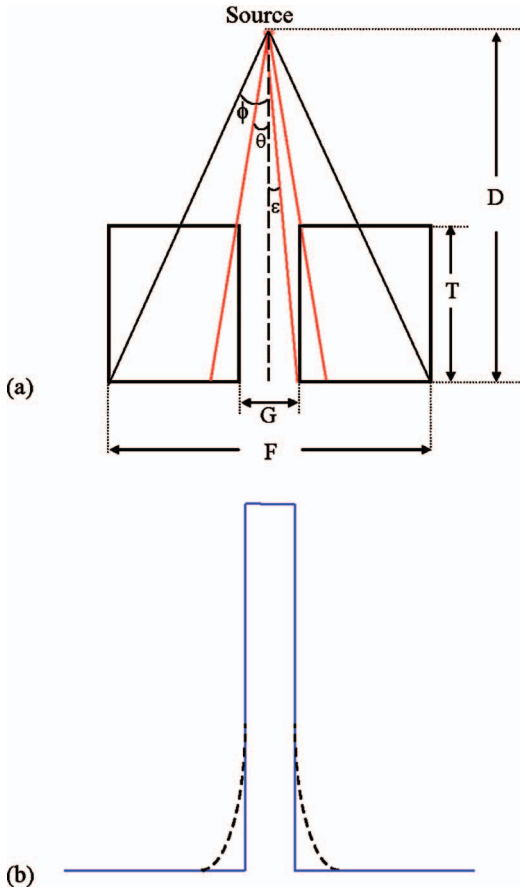

FIG. 1. (a) Schematic illustration (not to scale) of a cross-sectional view of a slit placed under a linac source. The dashed line indicates the central axis of the beam. The angles ϕ, θ, and ε correspond to x-ray trajectories through various edges of the slit. For clarity, the x-ray trajectory that defines the angle ε is shown on only one side. (b) 1D profile of the x-ray signal obtained at the exit surface of the slit. Ideally, the signal should be a rect function, as indicated by the solid line. The dashed lines indicate deviation from the ideal characteristic due to edge-penetration from x-rays incident along straight-line trajectories having angles between ε and θ, and assuming no penetration of x rays having angles between θ and ϕ.

A. Transmitted radiation

The LSF characterizes the 1D impulse response of an imaging system. Thus, the portion of the x-ray beam transmitted through the slit, which constitutes the "input" to the imaging system, should closely resemble an impulse function. This, in turn, requires almost complete attenuation of incident photons that do not pass directly through the slit gap [i.e., photons that are incident at angles greater than ε in Fig. 1(a)]. However, such a large amount of attenuation, while highly desirable, requires the use of massive, high-density blocks. As discussed previously, practical considerations place limits on the size of the blocks that can be used to create the slit. Thus, for relatively compact slit designs, it is possible that a small but non-negligible amount of radiation [incident between angles θ and ϕ, Fig. 1(a)] will penetrate

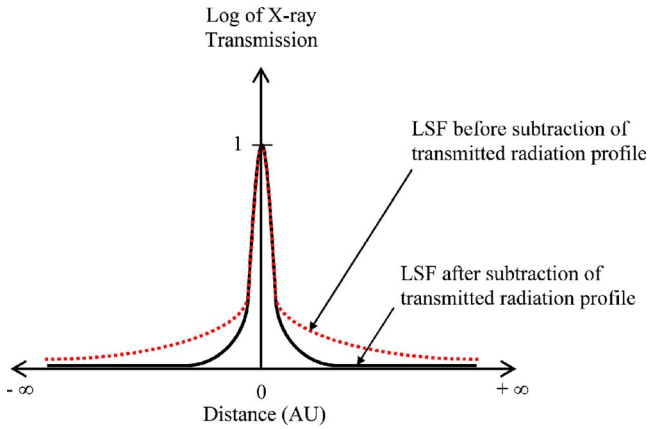

FIG. 2. Schematic depiction of the effect of transmitted radiation on the LSF baseline. The dashed and solid lines correspond to LSF values obtained before and after subtraction of the transmitted radiation profile, respectively. Distance from the beam central axis is indicated in arbitrary units. In order to better illustrate the differences between the LSF shape before and after subtraction, the x-ray transmission is shown on a "logarithmic" scale. Note that such subtraction can introduce a small reduction in the magnitude of the peak of the corrected LSF compared to that of the uncorrected LSF. This difference decreases as the amount of radiation transmitted through the solid block decreases; e.g., in the case of a block that completely attenuates the beam, no signal will be subtracted from the LSF peak. In the present study, due to the relatively low x-ray transmission exhibited by all the configurations examined, this effect is not observed in the MTF results shown in Figs. 4 and 7.

through the blocks. This radiation has two effects. First, due to the divergent nature of the incident x rays, the transmitted radiation results in a nonuniform beam profile at the x-ray exit surface of the slit. As shown in Fig. 2, a line spread function measured using such a beam will exhibit a distorted baseline, which in turn results in an underestimation of the MTF. In order to compensate for the effect of this distortion, the shape of the transmitted radiation profile can be estimated independently and subtracted from the LSF (Fig. 2). Such an independent estimate can be obtained by acquiring an image (under identical imaging conditions) of a solid, continuous block of the same material and dimensions as those of the slit. Alternatively, and perhaps more conveniently, the radiation profile may be estimated by imaging the slit after moving it laterally by a few millimeters so that the slit gap is sufficiently displaced from the beam central axis so as to prohibit unimpeded passage of x rays through the blocks. Furthermore, while this technique can largely rectify the distortion caused by x rays penetrating through the entire thickness of the blocks, corresponding to incident angles greater than θ but less than ϕ in Fig. 1(a), it cannot correct for the effect of partial penetration of x rays through the slit edges (as discussed in the following section), corresponding to angles less than θ but greater than ε.

A second effect caused by the penetrating radiation is an increase in the noise level observed in the baseline of the LSF. The presence of such noise can make it difficult to estimate the true value of the baseline, thereby resulting in a systematic error in the calculated MTF. In addition, high levels of baseline noise can obscure the true shape of the LSF, thus severely undermining the utility of the LSF, and thereby the MTF, as reliable quantifiers of the system impulse response. While, in principle, it may be possible to reduce such noise by increasing the amount of incident radiation, thereby allowing the use of more compact slits to make LSF measurements, it is important to examine the degree to which slit thickness can be reduced before the required dose (for acceptably low baseline noise levels) becomes so high as to be impractical.

B. Beam attenuation

From the standpoint of compactness, it is desirable that the material constituting the slit blocks exhibits very high attenuation per unit length. Consequently, megavoltage imaging slits are fabricated using blocks of high-density materials such as steel ($\sim 7.9\ \mathrm{g/cm^3}$) and tungsten ($\sim 19.3\ \mathrm{g/cm^3}$).

Another, more subtle effect pertaining to attenuation occurs due to beam penetration through the edges of the slit. As seen from Fig. 1, x rays that are incident at angles less than θ but greater than ε, pass partially through the block edges that form the slit gap. As a consequence of such partial penetration, the profile of the beam exiting the slit [see Fig. 1(b)] exhibits a deviation (dashed lines) from the ideal shape (solid line). This "blurred" input impulse function becomes convolved with the true line spread function of the imaging system, resulting in an overestimation of the degree of spatial spreading (and thereby an underestimation of the MTF) measured from the system. Therefore, the amount of attenuation provided by the blocks should be sufficiently high so as to minimize this effect. In addition, it can be seen from Fig. 1(a) [and from Eq. (2)] that, for a given distance between the source and the exit surface of the slit, the value of θ will diminish with decreasing thickness T of the metal block. Consequently, if the same amount of attenuation could be achieved using a thinner block (e.g., by choosing tungsten over steel), the beam profile at the exit surface of the slit will exhibit a smaller degree of deviation from the ideal shape shown in Fig. 1(b).

C. Other considerations

In addition to the issues discussed above, other major factors to be taken into account in the design and use of a slit for megavoltage imaging include the width of the slit gap, the distance between the x-ray source and the exit surface of the slit, and the field size at the exit surface. In principle, as the slit gap progressively decreases, the exiting beam more closely approaches an impulse function. This can be attributed to two effects; reduced beam width and a reduction in the amount of edge penetration due to a decrease in the angle θ [Fig. 1(a)]. In practice, due to the fact that the focal spot on the x-ray source has finite dimensions, it is desirable that the slit gap be chosen as thin as possible so that the finite size of the focal spot has a negligible effect on the MTF measurement. However, the benefits of decreasing the gap width are countered by the fact that slits with thinner gaps are increasingly more difficult to center with respect to the linac source.[2] In addition, decreasing the width of the slit gap re-

sults in a corresponding decrease in the magnitude of the signal transmitted through the gap. Consequently, the measured LSF exhibits a smaller peak-to-background ratio, which can make it difficult to estimate the true baseline of the LSF (required for accurate MTF determination) due to the presence of background noise.

Similar considerations also apply to the choice of the distance between the linac source and the x-ray exit surface of the slit. (The imager is usually placed in contact with this surface during LSF measurement. In such a case, this distance is also equal to the source-to-detector distance.) It can be seen from Fig. 1(a) that an increase in this distance will result in a corresponding decrease in θ and, therefore, in the effects due to the nonuniform profile of the transmitted radiation and edge penetration, both of which arise from beam divergence. However, placing the slit farther away from the source will also result in decreased signal, thereby increasing the noise in the baseline of the measured LSF. In addition, slit placement is often constrained by practical considerations; for instance, if there are physical restrictions on the positioning of a prototype imager or if an imager is attached to the treatment gantry.

The field size of the beam should be chosen so as to maximally utilize the area of the x-ray exit surface of the slit [Fig. 1(a)]. This ensures that the measured LSF has sufficiently long "tails" to enable accurate estimation of MTF values at lower spatial frequencies. In cases where the transmitted radiation profile is estimated by laterally displacing the slit by a few millimeters (Sec. II B), the area of the field should be chosen to be smaller than that of the x-ray exit surface of the slit. This ensures that when the slit is displaced from the central position, the x rays at the outer edges of the field still pass through the entire thickness of the blocks.

III. METHODS

A. Prototype slit

Previous megavoltage MTF measurements reported by our group on early prototype megavoltage AMFPIs were performed using a "traditional" slit design based on two 40 cm (thick) $\times$ 20 cm (long) $\times$ 5 cm (wide) steel blocks[6] (where thickness corresponds to the dimension along the path of the x-ray beam). The support and precise alignment of this massive slit relative to the AMFPI array required that the array be oriented in a vertical plane. This technique provided MTF values that were accurate and highly repeatable. However, the same slit and procedure could not be adapted for use with a new series of novel megavoltage AMFPI prototypes incorporating various forms of segmented converters—due to a practical need to keep the array in a horizontal plane while precisely registering the converter elements with the array pixels followed by precise orientation of the slit relative to the array+converter.[7,8] Therefore, in order to evaluate the imaging performance of these new prototype megavoltage AMFPIs, it was necessary to develop a less bulky slit.

Towards this objective, and based on the previously described technical considerations, a new prototype slit was designed (Fig. 3). The slit was composed of two tungsten blocks with precision-machined and polished opposing faces, each block having dimensions of $19 \times 8.5 \times 4.25$ cm^3, with the longest dimension (19 cm) positioned along the beam central axis, so as to constitute the "thickness" of the slit—considerably more compact than the earlier design. The blocks were separated by 0.01 cm thick stainless steel shims to form a long, narrow slit gap of dimensions $19 \times 8.5 \times 0.01$ cm^3. The slit was housed in a customized fixture that could be inserted into the accessory slot of the linac [Fig. 3(d)]. The four aluminum rods (made from aircraft-grade aluminum so as to provide high tensile strength) suspending the slit [Fig. 3(c)] were stabilized at regular intervals using high-strength, polycarbonate plates. (Polycarbonate was chosen so as to minimize the total weight of the assembly as well as to minimize x-ray scatter.) The dimensions of the blocks were chosen so as to ensure that the lateral dimensions of the slit were large enough to yield sufficiently long tails for measured LSFs (Sec. II C) and, at the same time, the total weight of the slit and the fixtures ($\sim$27 kg) was within acceptable limits for the accessory mount. (The considerably greater weight of the earlier slit, i.e., $\sim$63 kg, prohibited such incorporation with the accessory mount.) In this configuration, the x-ray exit surface of the slit was at a distance of 138 cm from the source. For each block, two small grooves ($\sim 1 \times 1 \times 4.25$ cm^3), on opposing sides, were machined $\sim$2.5 cm from the top surface. The two blocks were clamped together (after inserting the 0.01 cm shims) as shown in Fig. 3(b), and a polished steel plate was inserted in each "long groove" formed by the joining of the blocks. The entire assembly was connected to the aluminum rods via two through-holes machined into each steel plate [Fig. 3(a)]. In this arrangement, when the aluminum fixture was inserted in the accessory slot of the linac, the slit was suspended by the steel plates. The use of polished steel plates to suspend the slit allowed smooth, repeatable movements of the slit along the direction perpendicular to the slit gap. A dial indicator was placed in contact with one side of the slit in order to determine the exact amount of spatial displacement of the gap. This arrangement enabled relatively easy centering of the slit gap with respect to the linac source as well as precise lateral displacement of the slit gap away from the beam central axis in order to estimate the transmitted radiation profile. Moreover, due to the fact that the slit could be mounted into the linac accessory slot, it was possible to make MTF measurements with AMFPI arrays positioned in a horizontal plane.

Measurements were performed using the prototype slit in order to determine the MTF of a phosphor screen-based detector [Lanex Fast-B ($Gd_2O_2S:Tb$, 133 mg/cm^2) + 1 mm thick copper plate] coupled to an indirect detection, 508 μm pitch, active matrix photodiode array previously developed for megavoltage imaging applications.[6,14] The slit gap was centered with respect to the radiation source by iteratively determining the position that yielded the maximum signal through the slit. The imager, consisting of the x-ray detector and the active matrix array, was positioned such that the

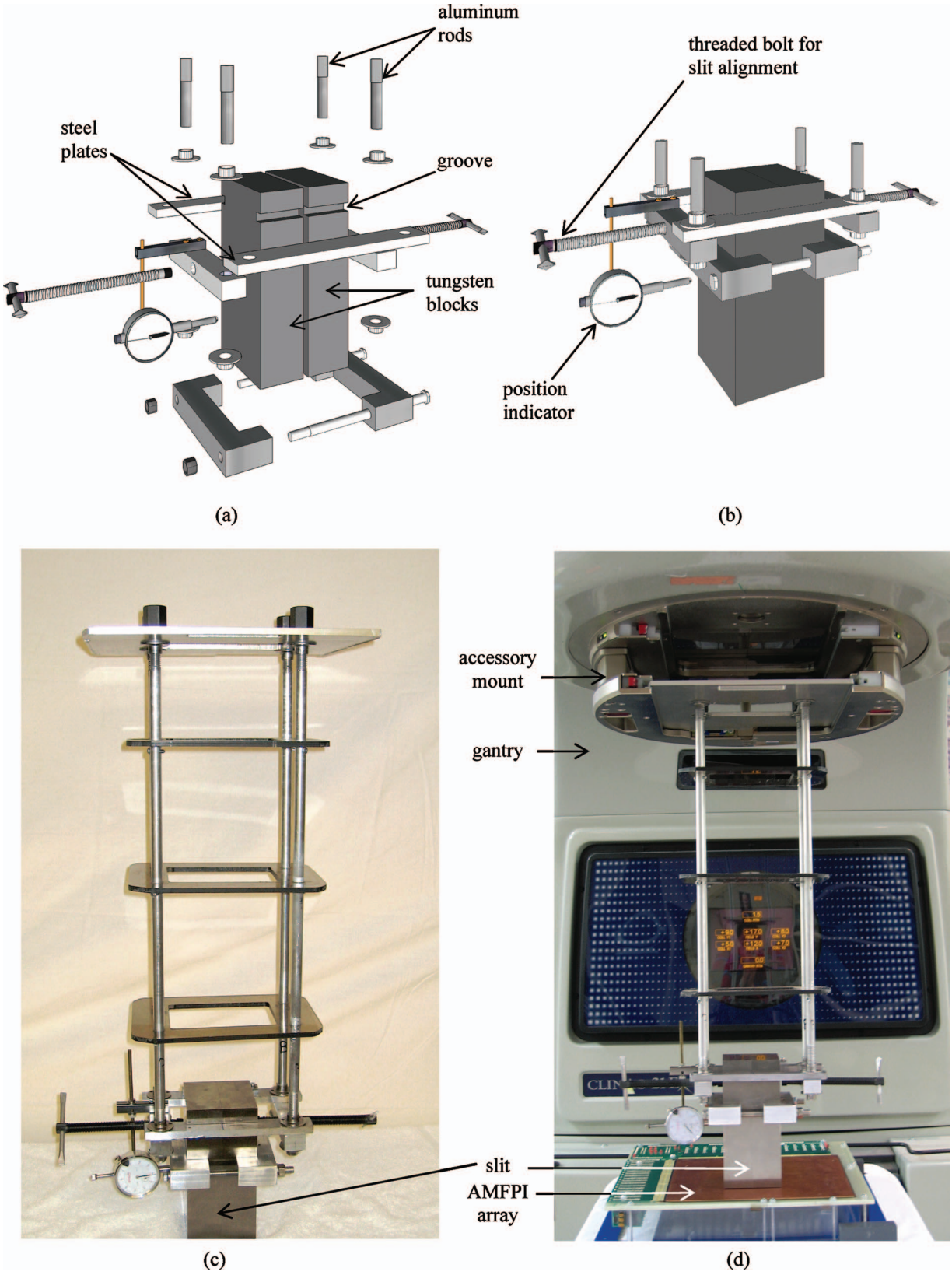

FIG. 3. Schematic (a) exploded and (b) assembled drawings of the prototype tungsten slit. (c) Photograph of the complete slit assembly. (d) Experimental setup for MTF measurement using the prototype slit attached to the accelerator accessory mount.

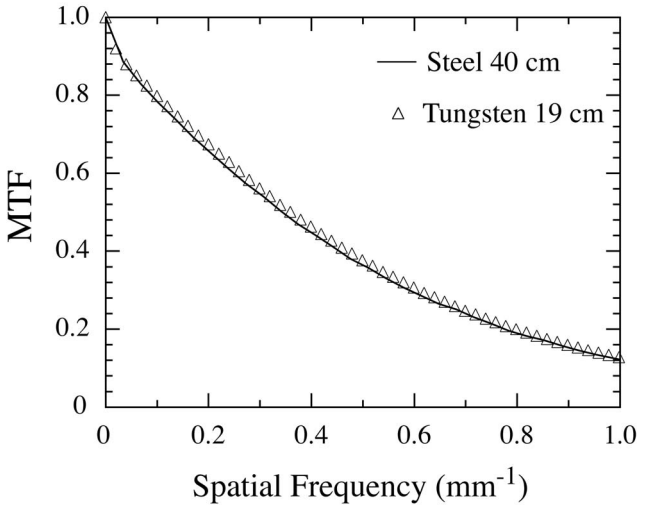

FIG. 4. Presampled MTF measured using the prototype slit (open symbols) at 6 MV from a 508 μm pitch, active matrix flat panel EPID based on a Lanex Fast-B screen+1 mm Cu. Also shown for comparison (solid line), are previously published MTF values (Ref. 6) for a similar megavoltage imager, obtained using a 40 cm thick steel slit.

detector was almost in physical contact with the x-ray exit surface of the slit. The field size was adjusted to be 6.5 $\times$6.5 cm^2 at the exit surface of the slit. Following the angled-slit technique for MTF determination of digital systems,[13] the linac collimator was rotated by $\sim$1.5° in order to orient the slit gap at a small angle with respect to the data line direction of the active matrix array.

Image frames were acquired by operating the imager in radiographic mode. (In radiographic mode, a single image frame is acquired after the linac delivers a programmed amount of radiation.[15,16]) A total of ten images of the slit (with the gap centered with respect to the source, as described above), each at 1 monitor unit (MU), were acquired. (For the calibration established by our clinic for this linac, 1 MU corresponds to a dose of 0.8 cGy deposited in water at a source-to-detector distance equal to 100 cm, with 10 cm overlying water, for a field size of 10$\times$10 cm^2 at the isocenter, i.e., at 100 cm.) In order to correct for potential distortions in the LSF caused by transmitted radiation (Sec. II B), ten images of the radiation profile, each at 1 MU, were acquired after displacing the slit gap $\sim$0.5 cm away from the center of the beam. Gain and offset corrections were applied to each image in each data set. The corrected images in each data set were then averaged to yield one slit image and one image of the radiation profile. Subsequently, the averaged radiation profile image was subtracted from the averaged slit image and the LSF was estimated according to the angled-slit technique. The absolute value of the Fourier transform of the LSF yielded the one-dimensional, presampled MTF of the imaging system.

B. Monte Carlo studies

The fabrication of a compact slit and the consequent simplification of the MTF measurement procedure prompted two interesting questions: Can slit design be made even more compact (e.g., by using thinner blocks); and, what effect would such increased compactness in design have on measurement accuracy? In order to investigate these issues, a novel theoretical methodology was developed. The methodology was based on Monte Carlo simulation of x-ray transport through a variety of hypothetical slit configurations. This approach serves as a powerful tool that can be used to examine virtually any design parameter. In the present work, due to practical constraints, only two design parameters, slit material and block thickness, which were considered to be the most important, were studied.

Monte Carlo simulations of x-ray transport were performed for slit designs based on various thicknesses of steel (from 10 to 40 cm) and tungsten (from 5 to 19 cm) using the BEAMnrc and DOSXYZnrc Monte Carlo codes.[17] The slit configurations examined in this study were chosen so as to be representative of designs described previously by our group and others.[3,6–8,11] It should be noted, however, that the total number of configurations that could be examined were limited by the available computational resources.

The simulations were performed in two stages, with a goal of estimating the MTF corresponding to the spatial spreading in the energy absorbed within a detector based on a $Gd_2O_2S:Tb$ phosphor screen of density 133 mg/cm^2, coupled to a 1 mm thick overlying Cu plate—similar to the detectors used in conventional megavoltage AMFPIs.[18] Note that, unlike the measured MTFs described in the previous section, these Monte Carlo-based MTFs do not account for spatial spreading of optical photons within the detector. (Detailed modeling of optical transport within the phosphor screen was outside the scope of this work.) It is known that optical spreading reduces the noise arising from energy absorption within a detector.[19] Therefore, for a given slit design, the noise level observed in an empirically determined MTF will be likely lower than that observed in the corresponding, simulated, "radiation-only" MTF.

In the first stage, the "impulse input" generated at the x-ray exit surface of a slit was estimated for each slit configuration using the BEAMnrc user code. The simulation geometry was similar to that shown in Fig. 1(a). For simplicity, the linac was modeled as a point source based on a 6 MV photon spectrum.[20] Thus, the effects of x-ray scatter from the linac head, the flattening filter, etc., were not considered in this study. In our current and previous[6–8] experience with megavoltage MTF measurement, these effects have not appeared to make any significant contribution to the accuracy of MTF estimation. The slit was modeled as two identically sized blocks separated by a 0.01 cm wide gap. Each block had dimensions of $T\times10\times5$ cm^3 (steel) and $T\times8.5\times4.25$ cm^3 (tungsten), where T is the block thickness along the beam central axis. (The lateral dimensions for the tungsten configurations were chosen to be slightly smaller than those of steel in order to save computational time. Note, however, that this difference in lateral dimensions has a negligible effect on LSF results between the two materials due to the fact that tungsten exhibits significantly more stopping

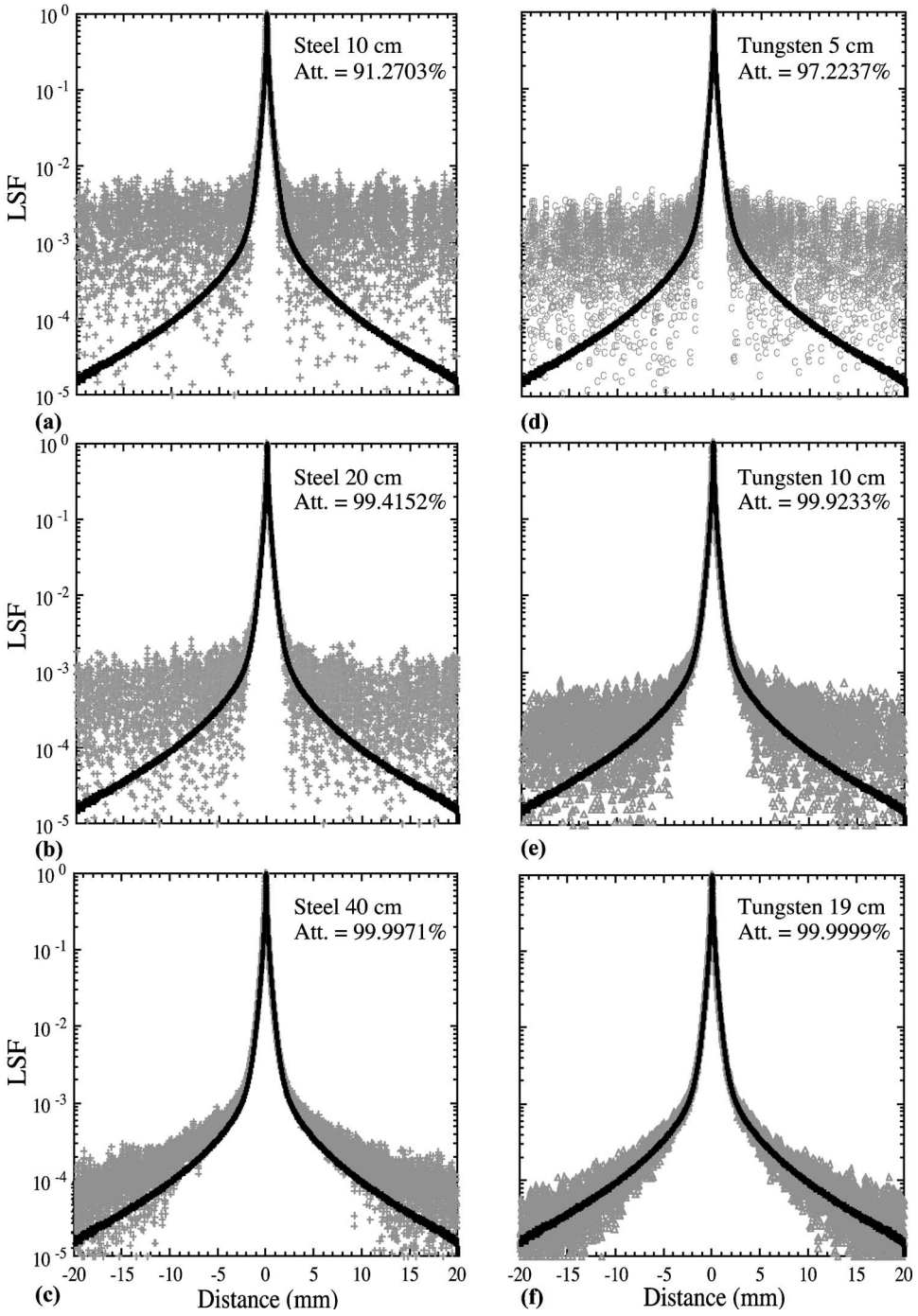

FIG. 5. Line spread functions obtained from Monte Carlo simulations of the energy absorbed, from a 6 MV photon spectrum, within a $Gd_2O_2S:Tb$ (133 mg/cm^2) phosphor screen, with an overlying layer of 1 mm copper. LSFs are shown (gray symbols) for slit designs based on (a) 10, (b) 20, and (c) 40 cm thick steel, and (d) 5, (e) 10, and (f) 19 cm thick tungsten blocks. For comparison, the LSF obtained using a mathematically defined parallel beam, and the same simulation parameters, is superimposed (black symbols) on each slit-based LSF. Finally, the amount of attenuation (calculated from phase-space files) suffered by a 6 MV photon beam spectrum passing through a continuous block of the specified type and thickness of material is also given in each case.

power than steel.) The field size of the incident radiation was chosen so as to correspond to an area of 6.5×6.5 cm^2 at the x-ray exit surface of the slit, which was defined to be at a distance of 130 cm from the source. This field size ensured that the resulting LSFs had sufficiently long tails. The cutoff energies for electron and photon transport were specified as 0.521 MeV (corresponding to a kinetic energy of 0.01 MeV) and 0.005 MeV, respectively. Thirty six billion incident photon histories were used for each simulation. For the aforementioned geometry, the photon fluence (at the slit exit surface) represented by this number is approximately equivalent to that from 1 MU delivered by a Varian linac.[6,20] In order to estimate the transmitted beam profile (Sec. II A), simulations were also performed for continuous slabs corresponding to each slit configuration, using identical dimensions and simulation parameters. The output at the exit surface of each slit (or slab) was saved in the form of "phase-space files," which contain information regarding the spatial location, charge, energy, and the direction of propagation for each particle crossing a user-specified plane.[17] The simulations were performed on a parallel computing cluster employing 320, 64-bit, Opteron™ 244 CPUs, each operating at 1.8 GHz. The total CPU time required per slit+slab combination ranged

from 6.25×10^3 to 46×10^3 h, corresponding to the least-attenuating (10 cm steel) and the most-attenuating (19 cm tungsten) configurations, respectively.

In the second stage, simulations were performed in order to estimate the spread of the absorbed energy within a detector using the DOSXYZnrc user code. Each of the phase-space files generated above was used as an incident x-ray source in DOSXYZnrc. The source was incident on a 10×4 cm^2, Gd_2O_2S:Tb phosphor screen+1 mm Cu detector described above. The absorbed energy was scored in the layer corresponding to the screen along a 5×4 cm^2 rectangular area in the center of the detector, with the shorter dimension of the area perpendicular to the narrow slit formed on the detector plane by the incident beam. The area was divided into 8000 voxels, each having a surface area of 5×0.0005 cm^2, in order to ensure sufficient sampling of the spatial spread of the absorbed energy, and a thickness equal to 360 μm—a value representative of a Lanex Fast-B screen.[6] The effect of the nonuniform transmitted radiation profile (Sec. II B) was removed from the 2D energy distribution of each slit configuration by subtracting the energy distribution obtained from the corresponding slab. Subsequently, the LSF was obtained from the energy deposition scored along the central area as a function of spatial location. The MTF was calculated from the absolute value of the 1D Fourier transform of the LSF. Note that, unlike the empirically determined LSFs described in Sec. III A, these Monte Carlo-based LSFs (and the corresponding MTFs) are determined for a "continuous" phosphor screen and therefore do not include the effect of a finite pixel aperture.

In order to determine how closely the LSF values obtained using each slit approach those obtained from an ideal input, a "gold standard" LSF was calculated. This gold standard consisted of the absorbed energy LSF determined through a separate DOSXYZnrc simulation that used a mathematically defined parallel beam having a width of 0.01 cm (equal to the slit gap) incident on an identical detector geometry. The beam was implemented using a built-in parallel, rectangular source model (ISOURCE 0) in the DOSXYZnrc code. Similar to the slit simulations, 36×10^9 incident histories were used so as to correspond to ~1 MU.

An important determinant of the reliability of calculated MTF values is the accuracy of determining the LSF baseline which, in turn, depends on the amount of noise present in the baseline relative to the magnitude of the LSF peak. The LSF peak-to-baseline noise ratio can therefore be employed as a useful figure of merit to compare the performance of various slit configurations. In order to further facilitate direct comparison between the various hypothetical slit designs (as well as with respect to the gold standard) all LSFs were normalized between zero and unity. Subsequently, for each LSF, baseline noise was calculated as the standard deviation (unitless, due to the normalization) in a total of 2000 data points—consisting of two sets of 1000 values, each set obtained from the "central region" of one half of the normalized LSF, away from the peak and edges.

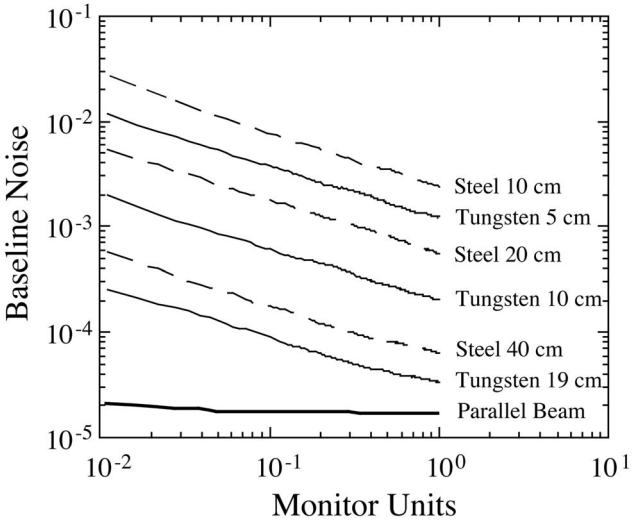

FIG. 6. Baseline noise (as quantified by the standard deviation) as a function of incident radiation for normalized LSFs obtained from the different slit designs examined in this study. (Note that due to the normalization of the LSFs between zero and unity, the baseline noise is unitless.) Dashed and solid lines represent results for designs based on steel and tungsten, respectively. For comparison, baseline noise for the LSF obtained using a parallel beam is also shown.

IV. RESULTS

A. Measurements

Figure 4 shows the MTF at 6 MV for a phosphor screen-based megavoltage AMFPI determined through measurements performed using the prototype, 19 cm thick, tungsten slit. Also shown are previously published MTF values for a similar imager using the earlier 40 cm thick steel slit. The MTF values obtained from the prototype slit exhibit a deviation, as quantified by the root mean square (RMS) difference, of ~1.2% with respect to the values obtained from the 40 cm thick steel slit. Such a close match demonstrates that, through the use of higher-density materials, significantly more compact slit designs may be achieved without compromising measurement accuracy.

B. Monte Carlo Studies

Figure 5 shows the line spread functions (normalized between zero and unity) obtained from the different slit designs. These LSFs correspond to the spatial spreading of the energy absorbed within a Gd_2O_2S:Tb phosphor screen for 1 MU of incident radiation from a 6 MV photon beam. For comparison, the LSF corresponding to a mathematically defined parallel beam input is superimposed on the results obtained from each slit configuration. As expected, the peak-to-background ratios increase with increasing beam attenuation. Notably, the LSF obtained from the 19 cm thick tungsten slit (which represents the prototype slit design) exhibits a higher peak-to-background ratio than that from the 40 cm thick steel slit. This further illustrates the benefits of using higher-density materials to increase the compactness of slit design without sacrificing accuracy. More importantly, the LSF

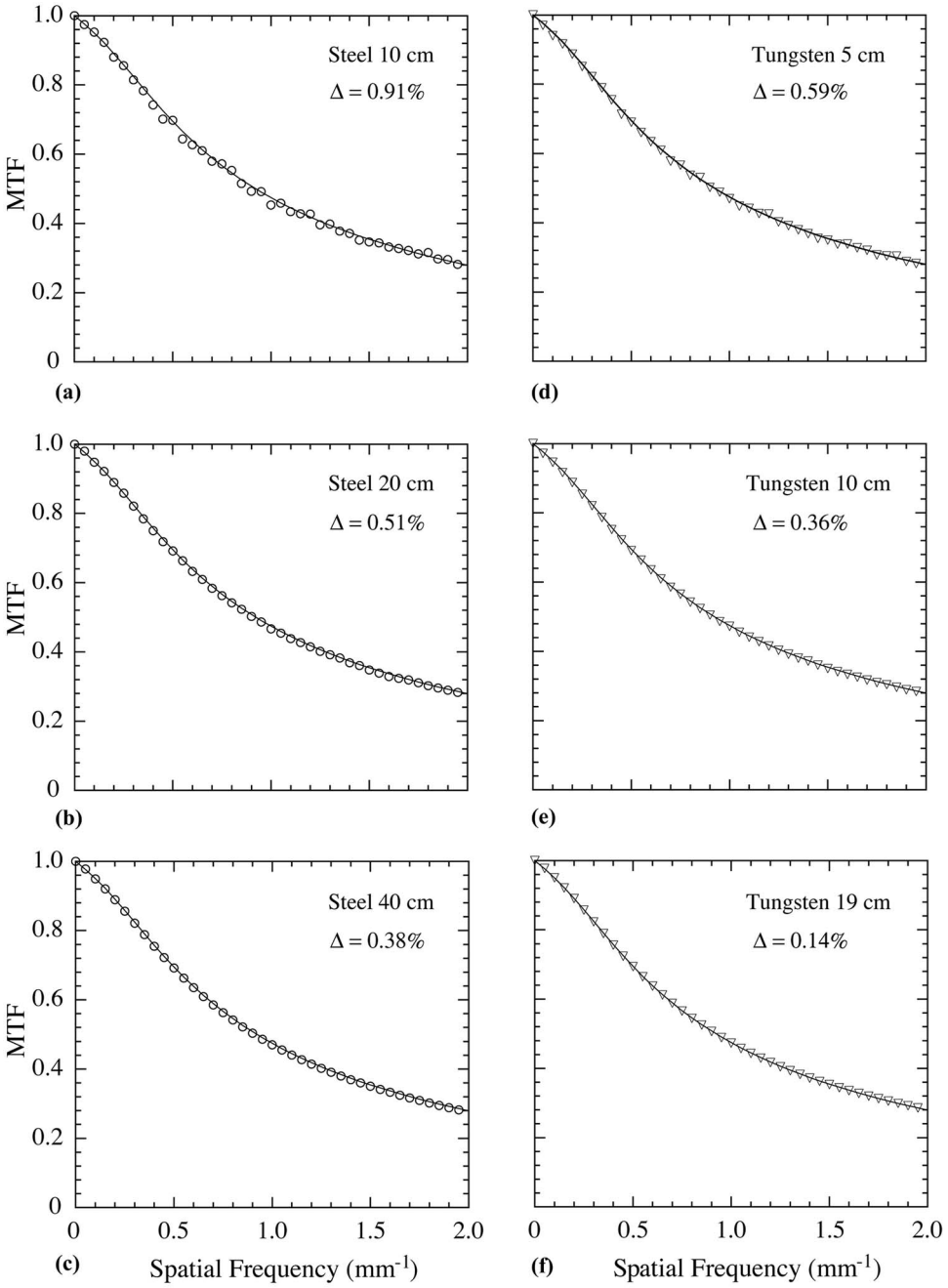

FIG. 7. One-dimensional modulation transfer functions for the different slit designs, calculated from the Monte Carlo-based LSFs shown in Fig. 5. The open symbols represent the calculated MTF values for slit designs based on (a) 10, (b) 20, and (c) 40 cm thick steel, and (d) 5, (e) 10, and (f) 19 cm thick tungsten blocks. The solid line in each graph represents the Monte Carlo-based MTF corresponding to a parallel beam input. The RMS difference (△) with respect to the parallel beam MTF is shown for each configuration.

from the 19 cm thick tungsten slit closely matches that from an "ideal input," i.e., the parallel beam, indicating that further increases in beam attenuation (e.g., through using thicker tungsten blocks) may not yield any significant improvements in the peak-to-background ratio.

Figure 6 shows the baseline noise in the LSF for each slit design as a function of incident radiation. For comparison, baseline noise as a function of incident radiation is also shown for the LSF, obtained from the parallel beam. As is the case of the peak-to-background ratios, the baseline noise also decreases with increasing beam attenuation. Furthermore, for each slit design, noise is observed to decrease with increasing incident radiation. However, the nature of these trends (note the logarithmic axes) suggests that, for a thinner slit to achieve the same levels of baseline noise as a thicker slit, the relative increase required in the amount of incident radiation would be very large. For example, in the cases of the two least-attenuating slit designs, based on 10 cm thick steel and 5 cm thick tungsten, it would require over 1000 MU to achieve baseline noise levels comparable to those achieved by the 40 cm thick steel and 19 cm thick tungsten-based designs at 1 MU—representing an increase of over three orders of magnitude.

Figure 7 shows one-dimensional MTFs calculated from the Monte Carlo-based line spread functions shown in Fig. 5 for the six slit designs examined in this study. In each case, the MTF values obtained using a slit appear to generally follow the trend described by the "ideal" curve correspond-

ing to a parallel beam input. In the cases of the 10 cm thick steel and 5 cm thick tungsten slits [Figs. 7(a) and 7(d), respectively], the calculated MTF values appear relatively noisy—most likely due to inadequate beam attenuation which increases the LSF baseline noise. The remaining four configurations yield MTF values that are very close to those obtained using a parallel beam. These results indicate that, despite exhibiting relatively high levels of LSF baseline noise, the 20 cm thick steel and 10 cm thick tungsten slit designs [Figs. 7(b) and 7(e), respectively] are capable of yielding measurement accuracy comparable to that obtained using the thicker designs [Figs. 7(c) and 7(f)].

V. DISCUSSION AND CONCLUSION

Empirical determination of MTF is routinely performed for "diagnostic" (i.e., kilovoltage) x-ray imagers.[1] While this metric is equally important for the performance characterization of megavoltage imagers, the various challenges associated with the megavoltage x-ray imaging environment make accurate measurement of the MTF a more daunting task. It is hoped that through the development of novel measurement tools such as the prototype slit described in this work, MTF measurement at megavoltage x-ray energies can be performed with relative ease without compromising accuracy.

As a result of the very large amount of computational resources required for simulating each slit design, the Monte Carlo studies were necessarily limited in scope, exploring only six different configurations based on two materials. Nevertheless, the Monte Carlo-based methodology developed in this work represents a powerful theoretical tool for the examination of existing as well as hypothetical designs. Furthermore, the results obtained from the present studies provide a number of valuable insights for practical slit design.

First, the LSF obtained from the slit design based on 19 cm thick tungsten blocks exhibits a peak-to-background ratio that is comparable to an ideally parallel beam. This result suggests an upper limit for the amount of beam attenuation required for the spectrum used in this study. In other words, further increases in attenuation are unlikely to yield any significant improvements in accuracy. Second, with the possible exception of the 10 cm thick steel slit [Fig. 7(a)], all of the designs examined in this study yield MTF values that closely follow the MTF obtained from a parallel beam, indicating that slit design may be made even more compact than the prototype without significantly reducing measurement accuracy. This result also serves as independent validation of MTF measurements reported in the literature using similar slit designs.[3,6–8,11] However, while the compact slits described in this study yield reasonably accurate estimates of MTF at 6 MV, it is worthwhile to note that higher levels of attenuation may be required for measurements with more energetic beams.

In summary, significant reduction in the bulkiness of the slit makes it easier to accurately determine the MTF under megavoltage x-ray imaging conditions. The availability of such convenient tools is expected to prove highly useful in the characterization of conventional, as well as novel, prototype megavoltage imagers.

ACKNOWLEDGMENTS

The authors would like to thank Alan Young for engineering support in the design and fabrication of the prototype slit and creation of the drawings in Fig. 3. We would like to express our appreciation to Wayne Keranen for setup and administrative support of the parallel computing cluster. We are grateful to Yi Wang for assistance with the figures and to Kwok Lam, Qihua Zhao, and Hong Du for providing valuable comments. This work was supported by Grant No. RO1 CA51397 from the National Institutes of Health.

[a]Author to whom correspondence should be addressed.

[1]J. T. Dobbins, "Image quality metrics for digital systems," in *Handbook of Medical Imaging*, edited by J. Beutel, H. L. Kundel, and R. L. Van Metter (SPIE, Bellingham, Washington, 2000), pp. 163–222.
[2]R. T. Droege, "A megavoltage MTF measurement technique for metal screen-film detectors," Med. Phys. **6**, 272–279 (1979).
[3]P. Munro, J. A. Rawlinson, and A. Fenster, "Therapy imaging: A signal-to-noise analysis of metal plate/film detectors," Med. Phys. **14**, 975–984 (1987).
[4]P. Munro and D. C. Bouius, "X-ray quantum limited portal imaging using amorphous silicon flat-panel arrays," Med. Phys. **25**, 689–702 (1998).
[5]P. Munro, J. A. Rawlinson, and A. Fenster, "Therapy imaging: A signal-to-noise analysis of a fluoroscopic imaging system for radiotherapy localization," Med. Phys. **17**, 763–772 (1990).
[6]Y. El-Mohri, K.-W. Jee, L. E. Antonuk, M. Maolinbay, and Q. Zhao, "Determination of the detective quantum efficiency of a prototype, megavoltage indirect detection, active matrix flat-panel imager," Med. Phys. **28**, 2538–2550 (2001).
[7]A. Sawant, L. E. Antonuk, Y. El-Mohri, Y. Li, Z. Su, Y. Wang, J. Yamamoto, Q. Zhao, J. Daniel, and R. A. Street, "Segmented phosphors: MEMS-based high quantum efficiency detectors for megavoltage x-ray imaging," Med. Phys. **32**, 553–565 (2005).
[8]A. Sawant, L. Antonuk, Y. El-Mohri, Q. Zhao, Y. Wang, Y. Li, H. Du, and L. Perna, "Segmented crystalline scintillators: Empirical and theoretical investigation of a high quantum efficiency EPID based on an initial engineering prototype CsI(Tl) detector," Med. Phys. **33**, 1053–1066 (2006).
[9]J. P. Bissonnette, D. A. Jaffray, A. Fenster, and P. Munro, "Optimal radiographic magnification for portal imaging," Med. Phys. **21**, 1435–1445 (1994).
[10]T. Falco and B. G. Fallone, "Characteristics of metal-plate/film detectors at therapy energies. I. Modulation transfer function," Med. Phys. **25**, 2455–2462 (1998).
[11]F. Cremers, T. Frenzel, C. Kausch, D. Albers, T. Schonborn, and R. Schmidt, "Performance of electronic portal imaging devices (EPIDs) used in radiotherapy: Image quality and dose measurements," Med. Phys. **31**, 985–996 (2004).
[12]S. Rathee, D. Tu, T. T. Monajemi, D. W. Rickey, and B. G. Fallone, "A bench-top megavoltage fan-beam CT using CdWO4-photodiode detectors. I. System description and detector characterization," Med. Phys. **33**, 1078–1089 (2006).
[13]H. Fujita, D. Y. Tsai, T. Itoh, K. Doi, J. Morishita, K. Ueda, and A. Ohtsuka, "A simple method for determining the modulation transfer-function in digital radiography," IEEE Trans. Med. Imaging **11**, 34–39 (1992).
[14]L. E. Antonuk, Y. El-Mohri, W. Huang, K.-W. Jee, J. H. Siewerdsen, M. Maolinbay, V. E. Scarpine, H. Sandler, and J. Yorkston, "Initial performance evaluation of an indirect-detection, active matrix flat-panel imager (AMFPI) prototype for megavoltage imaging," Int. J. Radiat. Oncol., Biol., Phys. **42**, 437–454 (1998).
[15]L. E. Antonuk, J. Yorkston, W. Huang, H. Sandler, J. H. Siewerdsen, and Y. El-Mohri, "Megavoltage imaging with a large-area, flat-panel, amorphous silicon imager," Int. J. Radiat. Oncol., Biol., Phys. **36**, 661–672 (1996).

[16]L. E. Antonuk, Y. El-Mohri, J. H. Siewerdsen, J. Yorkston, W. Huang, V. E. Scarpine, and R. A. Street, "Empirical investigation of the signal performance of a high-resolution, indirect detection, active matrix flat-panel imager (AMFPI) for fluoroscopic and radiographic operation," Med. Phys. **24**, 51–70 (1997).
[17]J. A. Treurniet, B. R. B. Walters, and D. W. O. Rogers, "BEAMnrc, DOSXYZnrc and BEAMDP GUI User's Manual," NRC Report PIRS 0623(rev B), 2001.
[18]L. E. Antonuk, "Electronic portal imaging devices: A review and historical perspective of contemporary technologies and research," Phys. Med. Biol. **47**, R31–R65 (2002).
[19]I. Cunningham, "Applied linear-systems theory," in *Handbook of Medical Imaging*, edited by J. Beutel, H. L. Kundel, and R. L. Van Metter (SPIE, Bellingham, Washington, 2000), pp. 79–159.
[20]D. Sheikh-Bagheri, "Monte Carlo study of photon beams from medical linear accelerators: Optimization, benchmark and spectra," Dept. of Physics, Carleton University, 1999.